Sustainable Energy, Grids and Networks 46 (2026) 102156

Contents lists available at ScienceDirect

Sustainable Energy, Grids and Networks

journal homepage: www.elsevier.com/locate/segan

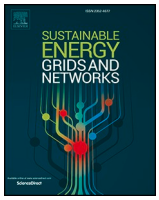

A novel statistical framework for modeling active and reactive power flexibility in a balancing service provider's distributed energy resource portfolio

Edoardo Daccò [a,*], Davide Falabretti [a], Claudio Cañizares [b]

[a] Department of Energy, Politecnico di Milano, Via La Masa 34, Milano 20156, Italy
[b] Department of Electrical and Computer Engineering, University of Waterloo, 200 University Avenue West, Waterloo, Ontario N2L 3G1, Canada

ARTICLE INFO

Keywords:
Active distribution network
Aggregation
Balancing service provider
Distributed energy resources
Feasible operation region
Flexibility services

ABSTRACT

Distributed energy resources can play a crucial role in providing ancillary services at both transmission and distribution level, aimed at enhancing load balancing and supporting overall grid resilience and stability. However, the effective utilization of these services remains challenging for Balancing Service Providers, as the actual capabilities of the regulating distributed energy resources are often partially known. To address this challenge, this paper introduces a new and comprehensive statistical framework for flexibility modeling and characterization, based on the concept of active-reactive power feasible operating regions that properly account for the distributed energy resource technical limits and uncertainty. The proposed novel statistical algorithm evaluates the flexibility contribution of both individual distributed energy resources and their aggregation, by incorporating into the formulation their service provision costs and reliability information. The derived feasible operating regions are particularly valuable for Balancing Service Providers, which can leverage them to assess market potential, optimize participation strategies, and design portfolios of contracted resources in an aggregated and probabilistic framework. Numerical results, based on illustrative case studies and real-world distributed energy resource data from the city of Milan, confirm the effectiveness of the proposed framework for determining, from a probabilistic standpoint, their ancillary service potential.

1. Introduction

The rapid growth of Distributed Energy Resources (DERs), largely driven by worldwide decarbonization initiatives such as the European Union's green initiatives [1] and [2], presents significant challenges for both Distribution System Operators (DSOs) and Transmission System Operators (TSOs). If not effectively managed, DERs can interfere with grid operations, which may result in undesirable operating conditions, thus hindering the grid operators' task in maintaining a secure and reliable network. On the other hand, if properly controlled, DERs could benefit both DSOs and TSOs [3]. In accordance with European and Member State regulations [4], [5], [6], both DSOs and TSOs can now procure flexibility services offered by DERs to improve quality of service and security of supply. In this context, Flexibility Providing Units (FPUs), defined as a subset of DERs and Demand Response (DR) units, can adjust their operating setpoint to provide flexibility services to grid operators such as active power modulation, frequency reserve, and voltage regulation [7], [8]. However, DER units are often equipped with metering infrastructures that offer limited performance: real-time information, for instance, is frequently unavailable. This limitation may prevent the BSP from fully exploiting the potential of DERs, as the actual state of the regulating unit remains unknown and, consequently, its real capability to respond to a power regulation request becomes uncertain [9], [10]. To overcome this issue, it is important to enhance the observability and controllability of DERs at Low-Voltage (LV) and Medium-Voltage (MV) grid levels, as the number of controllable units continues to rise. For this purpose, P-Q charts have been identified as a useful mechanism to monitor the amount of flexibility that FPUs can provide [11]. These charts are particularly useful because they can offer an estimation, based on, for example, optimization [12], neural networks [13], or statistical procedures [14], of the active and reactive power contributions of FPUs connected to Active Distribution Networks (ADNs). The concept of P-Q charts has also been proposed as an effective tool for information exchange at the TSO-DSO interfaces, especially in the context of increasing penetration of DERs and the decentralization of

* Corresponding author.
E-mail addresses: edoardo.dacco@polimi.it (E. Daccò), davide.falabretti@polimi.it (D. Falabretti), ccanizares@uwaterloo.ca (C. Cañizares).

https://doi.org/10.1016/j.segan.2026.102156
Received 4 September 2025; Received in revised form 19 December 2025; Accepted 12 February 2026
Available online 18 February 2026

Nomenclature

Acronyms

ADN	Active Distribution Network
BESS	Battery Energy Storage System
BSP	Balancing Service Provider
CCC	Circular Capability Curve
CDF	Cumulative Distribution Function
CHP	Combined Heat and Power
DER	Distributed Energy Resource
DPI	Delivery Performance Index
DR	Demand Response
DSO	Distribution System Operator
FOR	Feasible Operating Region
FPU	Flexibility Providing Unit
LCC	Limited-circular Capability Curve
HV	High-Voltage
LV	Low-Voltage
MPPT	Maxum Power Point Tracking
MV	Medium-Voltage
PAR	Probability Aggregated Region
PV	Photovoltaic
RCC	Rectangular Capability Curve
SoC	State of Charge
SCC	Synchronous Capability Curve
TCC	Triangular Capability Curve
TSO	Transmission System Operator

power generation [11], [15].

More recently, P-Q charts have been further expanded to incorporate dynamic operating constraints, such as resource capacity, ramp rates, and service duration [16], [17], which are referred to as Feasible Operating Regions (FORs). In this regard, [18] provides an extensive comparison and validation of several random sampling and optimal power flow methods for computing FORs in ADNs, with research studies being classified into three main categories. The first category includes deterministic FORs based on optimal power flow formulations, through with feasibility regions being derived from explicit network models and static capability limits. For instance, the authors in [19] combine AC optimal power flow and cooperative game theory to trace and value DER flexibility in ADNs, helping DSOs to identify critical units and avoid unreliable operating regions. In [20], FORs are developed using a linear optimization model that also considers tap changers at High-Voltage (HV)/MV substations. FORs can also account for network constraints as in [21] and [22], in which voltage and current violations are considered in nodes and branches, respectively. This enables the use of FORs for monitoring and controlling ancillary services, thereby facilitating system operation enhancements, such as congestion management [23]. The authors in [24] proposed a decentralized and hierarchical approach for the practical implementation of coordinated vertical flexibility on multiple voltage levels, considering FORs at the interface between adjacent networks or voltage levels. In all these papers, FORs are primarily focused on the flexibility contributions at HV/MV interfaces, especially from a DSO's perspective, where all information about the network's structure is available. However, none of these works examine how the concept of FORs can be extended to support BSPs, which typically operate with limited observability of DER's capabilities and operational constraints. In particular, existing approaches do not provide BSP-oriented tools for assessing DER flexibility from both aggregated and probabilistic perspectives, thereby facilitating their effective participation in local and system-wide flexibility markets, as proposed in the present study.

The cost of deviation from the current dispatch point may significantly influence the potential of FORs to participate in various markets. In this regard, a second category of studies integrates cost terms into the definition of flexibility. Thus, in [25] and [26], the cost of power diversion is attributed to several factors, including the additional cost of fuel, variable maintenance costs (e.g., ramping fatigue), lost-opportunity costs (e.g., limiting active power to supply reactive power [27]), and power buyback in the case of storage. The costs that DSOs are willing to pay for the activation of flexibility services are represented with several overlapping P-Q curves in [28]. A similar approach is presented in [29], in which the authors introduce a method for monetizing FORs at the TSO-DSO interface by using cost structures, applying a mixed-integer linear program for cost-optimal disaggregation of flexibility demands among units. However, in these studies, service provision cost is treated merely as an additional model parameter that further constrains FORs, without accounting for the specific characteristics or operational limitations of individual FPUs, as proposed in this work.

In the existing approaches to estimate FORs, it is assumed that FPUs are available to fully provide the required flexibility service, regardless of the DER's actual conditions. This is not reasonable in practical applications, as the reliability of each distributed generator to deliver the requested active and reactive output is uncertain, especially at LV levels, where the acquisition of real-time measurements and operating points is often a challenge. Thus, the third category of research work comprises probabilistic and uncertainty-aware FORs, which incorporate variability in DER behavior in their formulations. In this context, the authors in [30] propose probabilistic reactive power capability charts, which represent reactive power support limits of distribution systems as families of random variables with their associated probabilistic density functions. This approach identifies different levels of flexibility with related uncertainties; however, the flexibility contribution of each DER is concealed in this case. In [31], the reliability of the DERs is described as a variable coefficient between 0 and 1 in their P-Q charts; however, the paper does not discuss how this coefficient can be identified for each distributed resource. Uncertainty is treated as a confidence interval that reduces the feasible region in [32], making the aggregation of FPUs more conservative. These papers assume that BSPs can monitor all DERs in a coordinated and centralized manner during operation, which often is not the case in practice. As a result, existing methods that rely on the real-time measurement of DER operating points may have a limited applicability in real life, particularly at the LV level, which is an issue considered in this paper. To further highlight the methodological gaps addressed in this work, Table 1 qualitatively summarizes the main differences between existing FOR approaches and the one proposed here, which indicates whether each approach includes or not a given modeling feature.

Based on the presented literature review, this paper proposes an innovative formulation of FORs, which captures the potential of individual FPUs to deliver ancillary services. In this regard, existing approaches typically require full network observability or rely on real-time operating conditions of DERs, which limit their applicability to BSP operational environments. In contrast, this work addresses how DERs' active and reactive flexibility can be represented in a probabilistic and aggregated manner under limited DER observability, to support BSP portfolio optimization and bidding strategies. To this purpose, the proposed FORs incorporate DER's provision costs and reliability, thereby providing a more accurate and comprehensive representation of flexibility services, encompassing both active power (upward and downward regulation) and reactive power (capacitive and inductive support) services. To this end, a statistical algorithm is developed to define and incorporate a novel reliability index in the FORs computation,

Table 1.
Comparison of existing and proposed FOR approaches.

Category	References	Data-driven	Probabilistic / reliability	Cost integration	Requires full grid model	Suitable for BSPs
Deterministic FOR approaches	[20], [21], [22], [23], [24]	N	N	N	Y	N
Cost-integrated FOR approaches	[25], [26], [27], [28], [29]	N	N	Y	Y	N
Probabilistic FOR approaches	[30], [31], [32]	Partially	Y	N	Y	N
Proposed Method	Current paper	Y	Y	Y	N	Y

highlighting the probability of individual FPUs or their aggregation to provide active and reactive power flexibility services as requested. The resulting regions allow modeling DER regulation capabilities without the complete knowledge of network operating conditions. For this reason, this method is particularly valuable for BSPs, which usually have partial or simplified knowledge of network topology and constraints, according to which they must estimate the feasible contribution of the contracted resources to ancillary services markets. Furthermore, service costs of the most common DERs in today's ADNs are also considered in the proposed FORs.

The key contributions of this work can be summarized as follows:

- A novel probabilistic framework for constructing FORs of individual FPUs is proposed, fully data-driven and capable of capturing static limits, dynamic operating constraints, and service-dependent costs. Unlike existing deterministic or OPF-based feasible-region approaches, the proposed formulation embeds provision reliability through probability distributions based on real measurements, and associates each point of the region with an explicit reliability index.
- The proposed approach includes an aggregation procedure that combines multiple individual FORs into Probabilistic Aggregated Regions (PARs), enabling BSPs to quantify the total active/reactive flexibility available from heterogeneous portfolios. The aggregation is based on a DPI-filtered Minkowski sum that preserves reliability information while ensuring computational tractability.
- A practical application is provided of the resulting FORs and PARs for BSP operations, such as market-potential assessment, portfolio optimization, and strategy refinement, demonstrating how the proposed methodology applies to cases where network information is limited or unavailable, in contrast with research studies that rely on distribution grid models or full observability. Thus, the presented technique is applied and validated using real DER data at an HV/MV substation of Milan's distribution network, confirming both the practicality and scalability of the approach, and demonstrating its effectiveness for large-scale BSP portfolios.

Note that the proposed approach focuses on developing improved FORs for BSPs to properly offer flexibility services on local or system-wise markets. In this context, the network structure and constraints are usually not known by service providers. However, if communicated by the DSO to the BSP, these constraints can be considered within the presented approach in a simplified manner [33].

The rest of the paper is organized as follows: The statistical algorithm used to identify the proposed probabilistic FORs of individual FPUs is discussed in Section II. Section III presents the determination of FORs considering the technical limits, such as capability curve and costs of DERs. In Section IV, the methodology to obtain the probabilistic aggregated FORs of sets of heterogeneous resources is presented. Section V demonstrates the effectiveness of the proposed framework through its application to several real DERs. Finally, the main conclusions and contributions of the paper are highlighted in Section VI.

2. Feasible operating region definition

FORs provide a snapshot of the active and reactive power flexibility that one or more FPUs can offer to the power system, facilitating grid management, as well as improving DER observability and their optimal exploitation. The FOR framework offers a significant advancement over traditional capability curves by capturing the aggregated flexibility of DERs. Indeed, unlike static P-Q curves, FORs can be dynamically updated in real time to reflect uncertainty in generation and demand, improving system coordination and market participation, and further facilitating communication among grid operators and stakeholders [34].

The FOR methods found in the literature require full knowledge of available FPUs capacity to assess the flexibility in distribution grids [21]; however, acquiring this information in real time is challenging and, in some cases, not even feasible. For this reason, this paper proposes the innovative concept of probabilistic FOR as a useful tool for BSPs to evaluate FPU's availability and reliability in offering ancillary services. A fundamental aspect of this approach is that it is not based on the DER's operational point at a given instant, which may not be available, especially in real time and at the LV level [23], but rather on their historical trends of active and reactive power outputs.

In more detail, the procedure proposed for identifying probabilistic FORs is based on the FPU's historical trends and technical limits, i.e., capability curves. Five different capability curves are considered in this study, defined in orange in Table 2, which are relevant to the generation technologies typically available in urban distribution networks [10], i.e., Photovoltaic (PV) and Combined Heat and Power (CHP); the green areas correspond to the combined limits when Battery Energy Storage Systems (BESSs) are considered. All capability regions but the latter correspond to inverter-based FPUs, such as PV power plants, for different ratings and voltage levels, while the Synchronous Capability Curve (SCC) corresponds to CHP plants, in which k_1 and k_2 are coefficients that depend on the generating unit's rated characteristics, i.e., maximum excitation current. In this table, S_n is the DER rated apparent power, and φ_{lim} is the phase angle corresponding to the power factor limit; these capability curves are consistent with the technical standards in place in many countries in the EU [35], [36]. For example, the operating region of a PV power plant at LV levels can be represented by the orange Triangular Capability Curve (TCC) illustrated in Table 2, which is typical of residential PV systems operating at unity power factor, i.e., $Q(t) = 0$.

The first step of the proposed algorithm consists in identifying the maximum active power service that the FPU can provide, either for upward $\Delta P_{+}^{\max}$ or downward $\Delta P_{-}^{\max}$ regulation. To this end, all the input active and reactive profiles $P(t)$ and $Q(t)$ correspond to the same data streams routinely collected from end users for billing and regulatory purposes, which guarantees that the entire measurement chain is subject to standard validation, consistency checks and quality-control procedures performed by network operators, ensuring an adequate level of data reliability for statistical analysis. Furthermore, if power measurements are unavailable, the BSP may choose to either discard the FPU, or proceed with reconstruction of missing points (e.g., through linear interpolation). These steps ensure that the probabilistic FORs reflect the true operational behavior of each DER and are not influenced by low-quality

Table 2
FPUs' capability curves.

Triangular Capability Curve (TCC)	
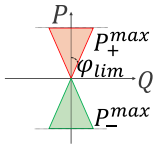	$Q_{\pm}^{max}(t) = \pm P(t) \cdot \tan \varphi_{lim}$
Rectangular Capability Curve (RCC)	
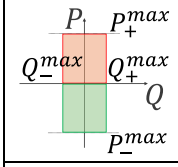	$Q_{\pm}^{max} = \pm S_n \cdot \tan \varphi_{lim}$
Limited-circular Capability Curve (LCC)	
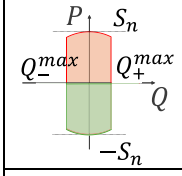	$Q_{\pm}^{max}(t) = \pm \min\left(S_n \cdot \tan \varphi_{lim}, \sqrt{S_n^2 - P(t)^2}\right)$
Circular Capability Curve (CCC)	
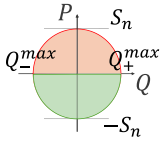	$Q_{\pm}^{max}(t) = \pm\sqrt{S_n^2 - P(t)^2}$
Synchronous Capability Curve (SCC)	
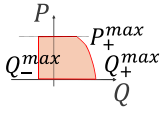	$Q_{-}^{max}(t) = -S_n \cdot \tan \varphi_{lim}$ $Q_{+}^{max}(t) = \min\left(\begin{matrix}\sqrt{S_n^2 - P(t)^2}, \\ \sqrt{{k_1}^2 - P(t)^2} - k_2\end{matrix}\right)$

measurements. Thus, given as an input $P(t)$, $\Delta P_{\pm}^{\max}(t)$ is calculated as:

$$\Delta P_{\pm}^{\max}(t) = P_{\pm}^{\max}(Q(t)) - P(t) \quad (1)$$

where the active power limits $P_{\pm}^{\max}$ are defined according to the FPU's capability curve and other technical limits, such as availability of the primary energy source, as a function of the reactive power exchanged before the regulation request. Since $\Delta P_{\pm}^{\max}(t)$ is the maximum active power variation that the FPU can provide according to its capability

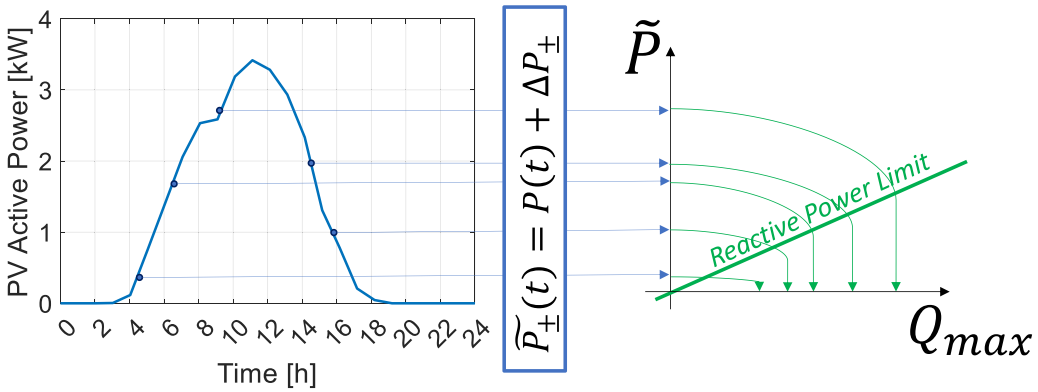

Fig. 1. Identification of maximum allowed reactive power variations based on the active power exchanged by the DER and its reactive power limits.

limits, all variations $\Delta P_{\pm}$ such that $|\Delta P_{\pm}| \leq |\Delta P_{\pm}^{max}|$ are also admissible. The sum of $\Delta P_{\pm}$ and $P(t)$ determines the FPU power exchanged as a result of the activation of an active power regulation, as follows:

$$\widetilde{P_{\pm}}(t) = P(t) + \Delta P_{\pm} \tag{2}$$

based on a generation sign convention, with $\sim$ representing power exchanges after flexibility activation. The maximum allowed reactive power variations $\Delta Q_{\pm}^{max}(t)$, based on $\widetilde{P_{\pm}}(t)$ and FPU's reactive power limits $Q_{\pm}^{max}$, can then be determined as follows, as illustrated in Fig. 1:

$$\Delta Q_{\pm}^{max}(t) = Q_{\pm}^{max}\left(\widetilde{\Delta P_{\pm}}(t)\right) - Q(t) \tag{3}$$

Consequently, the FPU is able to supply a maximum reactive regulation $\Delta Q_{\pm}$, so that $|\Delta Q_{\pm}| \leq |\Delta Q_{\pm}^{max}|$. The total amount of reactive power exchanged by FPU with the grid is then equal to:

$$\widetilde{Q_{\pm}}(t) = Q(t) + \Delta Q_{\pm} \tag{4}$$

It should be noted that the proposed approach prioritizes active power flexibility regulation over reactive one, given its higher value, as per [23]. Furthermore, the distribution of the admissible $\Delta P_{\pm}$ is modeled through data-driven probability density functions $f_{\pm}^{P}$, constructed directly from historical measurements over the ranges $[0, \Delta P_{+}^{max}]$ and $[\Delta P_{-}^{max}, 0]$. A similar approach can be used to obtain the probability density functions $f_{\pm}^{Q}$ over the intervals $[0, \Delta Q_{+}^{max}]$ and $[\Delta Q_{-}^{max}, 0]$. These functions represent the likelihood of a FPU in providing a specific amount $\Delta P_{\pm}$ ($\Delta Q_{\pm}$) of active (reactive) power regulation without imposing any parametric assumption on the probability distribution. This data-driven choice is motivated by the behavior of DERs, whose variability largely depends on seasonality, weather conditions, and operational schedules. By relying on data-driven probability distributions, the proposed approach avoids assumptions that are not supported by the physical behavior of the resources, ensuring that probabilistic FORs reflect realistic operating patterns. In contrast, models based on representative user behavior may fail to capture the specific operating characteristics of individual resources. Finally, both $f_{\pm}^{P}$ and $f_{\pm}^{Q}$ can then be integrated to get the following Cumulative Distribution Functions (*CDFs*):

$$CDF_{-}^{X}(x) = 1 - \int_{0}^{-\Delta x} f_{-}^{X}(t)dt \tag{5}$$

$$CDF_{+}^{X}(x) = 1 - \int_{0}^{\Delta x} f_{+}^{X}(t)dt \tag{6}$$

where $\pm\Delta x$ represent the amount of active or reactive power related to the corresponding service. CDFs are equal to 100 % if $\pm\Delta x = \Delta X_{\pm}^{max}$, i.e., $\Delta P_{\pm}^{max}$ or $\Delta Q_{\pm}^{max}$. Thus, $CDF_{\pm}^{X}$ describes the probability of a FPU providing a specific regulation $\pm\Delta x$. For example, Fig. 2 depicts the CDF_{-}^{P} of a PV system for a downward regulation service, where $CDF_{+}^{P} = 0$ given that PV units usually do not provide upward regulation, since they operate in Maximum Power Point Tracking (MPPT) mode.

Finally, active and reactive $CDF_{\pm}^{X}$ can be combined to compute the probabilistic FOR, as follows:

$$FOR = \begin{bmatrix} CDF_{+}^{P} \bullet CDF_{-}^{Q} & CDF_{+}^{P} \bullet CDF_{+}^{Q} \\ CDF_{-}^{P} \bullet CDF_{-}^{Q} & CDF_{-}^{P} \bullet CDF_{+}^{Q} \end{bmatrix} \tag{7}$$

where each block represents the matrix product between active and reactive CDFs, corresponding to the combined probability of providing active and reactive flexibility services. Thus, the probabilistic FOR, formulated as a matrix product of active and reactive power *CDFs*, represents a comprehensive and data-driven map of the FPU's capability to deliver flexibility services under uncertainty. Each element of the matrix quantifies the joint probability of the FPU providing a specific pair of active and reactive power variations, thereby enabling the assessment of not only whether a flexibility request is technically feasible, but also how likely it is to be successfully delivered. This approach allows BSPs and grid operators to move beyond deterministic representations and integrate probabilistic guarantees into their operational strategies.

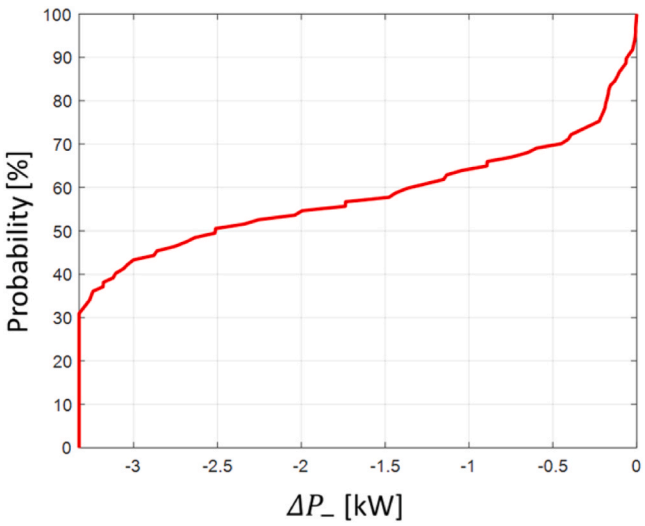

Fig. 2. Example of CDF_{-}^{P} for downward regulation of a PV panel.

3. FPU's technical limit modeling

As previously highlighted in Table 2, the technical limits of each FPU need to be accurately modeled to define their maximum contribution to flexibility services. To this purpose, the power measurements are collected at the point of common coupling between the prosumer and the external network, and at the generation and BESS terminals. Hence, P_{M1} and P_{M2} in Fig. 3, respectively, can be used to characterize the FPU's behavior from a probabilistic point of view.

Furthermore, depending on the type of resource and its operating conditions, the relevant flexibility service costs vary, which can significantly influence the FPU's potential to participate in the market. In the proposed formulation, the cost associated with each FPU represents the minimum remuneration required to enable a specific power variation to

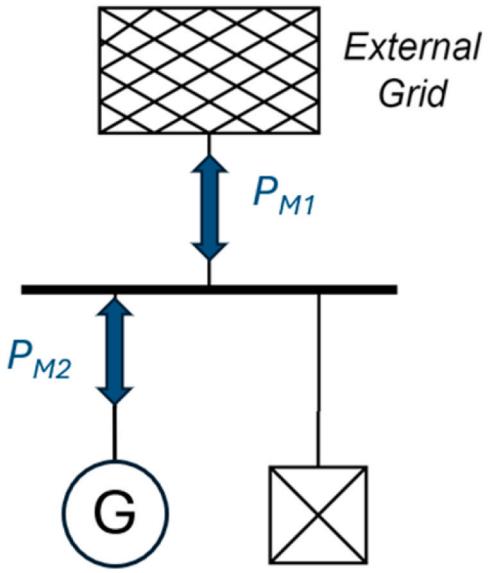

Fig. 3. Measurements used in the proposed approach.

deliver the required flexibility service. This definition is consistent with the internal operational constraints of each distributed resource (e.g., fuel consumption, thermal limits, efficiency losses, or battery degradation) and ensures that the cost dimension of the FOR reflects the true economic feasibility of delivering flexibility. In addition, note that, although the detailed design of local flexibility market remuneration mechanisms is outside the scope of this study, the proposed formulation is fully compatible with such schemes, as the flexibility service cost term has been defined to match the remuneration schemes offered in current DSO- and TSO-led procurement processes applied across Europe. These procurement processes are typically remunerated through activation-based rewards, and in some cases complemented by payments based on availability [37].

3.1. PV+BESS system

An illustrative diagram of this system is provided in Fig. 4, where the PV system is assumed to operate in MPPT mode, while the BESS is used to store the surplus PV production to deliver it later based on the user's demand (self-consumption maximization):

$$P_{M2}(t) = P_{BESS}(t) \quad + P_{PV}(t) \tag{8}$$

$$\widetilde{P_{BESS}}(t) = \quad P_{BESS}(t) + \Delta P_{BESS\pm} \tag{9}$$

$$\widetilde{P_{PV}}(t) = \quad P_{PV}(t) + \Delta P_{PV-} \tag{10}$$

$$\Delta P_{\pm} = \quad \Delta P_{BESS\pm} + \Delta P_{PV-} \tag{11}$$

$$P_{-}^{\max} \le \widetilde{P_{M2}}(t) \le P_{+}^{\max} \tag{12}$$

$$P_{\max}^{cha} \le \quad \widetilde{P_{BESS}}(t) \le P_{\max}^{dis} \tag{13}$$

Hence, in this case, P_{M2} is given by the mutual active power contribution of the BESS and the PV system, P_{BESS} and P_{PV}, respectively in (8). The flexibility service $\Delta P_{\pm}$ is provided by the BESS in (9), but, if cost-effective, the PV power plant can also provide downward regulation through curtailment in (10). Thus, both regulating resources can cooperate to supply the service required by the grid in (11). Eq. (12) describes the FPU's power limits $P_{\pm}^{\max}$ during flexibility activation, depending on the specific capability curve of the power plant depicted in orange and green colors for TCC, RCC, LCC, and CCC in Table 2. Finally, in (13), the maximum charging and discharging power of the BESS $P_{\max}^{cha}$ and $P_{\max}^{dis}$, respectively, are considered.

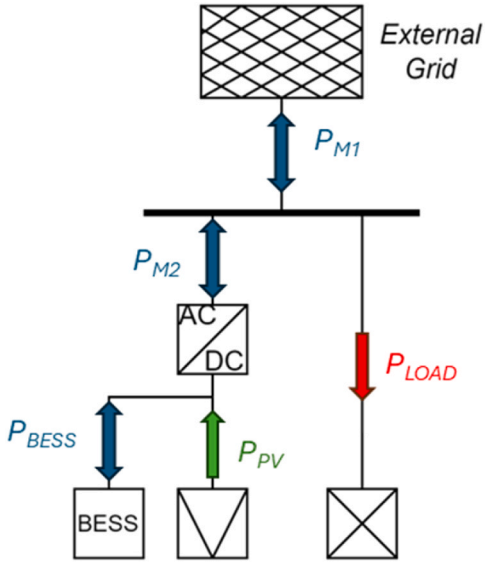

Fig. 4. PV+BESS system.

Besides active power limits, the BESS energy constraints must be considered as follows:

$$\widetilde{\Delta E} = \begin{cases} \dfrac{\widetilde{P_{BESS}}(t)}{\eta_{BESS}} & \Delta t \quad \forall \widetilde{P_{BESS}}(t) \ge 0 \\ \widetilde{P_{BESS}}(t)\,\eta_{BESS} & \Delta t \quad \forall \widetilde{P_{BESS}}(t) < 0 \end{cases} \tag{14}$$

$$\widetilde{SoC}(t+1) = \widetilde{SoC}(t) + \quad \frac{\widetilde{\Delta E}}{E_n} \tag{15}$$

$$SoC^{\min} \le \widetilde{SoC}(t+1) \le SoC^{\max} \tag{16}$$

where (14) represents the energy flexibility provision of the BESS $\widetilde{\Delta E}$ as a result of a behind-the-meter service request (self-consumption increase). The $\widetilde{SoC}$ after the activation of the flexibility service in (15) cannot exceed its minimum and maximum limits $SoC^{\min}$ and $SoC^{\max}$, respectively, as per (16). In these equations, E_n is the BESS net energy capacity, η_{BESS} is the charging/discharging BESS efficiency, and Δt is the flexibility service duration; for the sake of simplicity, the same efficiency is assumed for both charging and discharging.

Assuming a worst-case scenario for the BESS in which both upward and downward regulations lead to a reduction of the PV power self-consumed by the prosumer, the cost for the user resulting from the BESS service provision is equal to the loss of earnings associated with the decrease in PV power. In addition, the effects on battery degradation must also be considered, since, depending on the circumstances, the ancillary service provision would impact the BESS life compared to the scenario in which no regulation is provided. Thus, the service provision costs can be modeled as follows:

$$C_u = |\Delta P_{\pm}| \left(p_{buy} - p_{sale}\right) + C_{BESS} \tag{17}$$

where C_{BESS} accounts for the BESS energy charge/discharge costs, which can be calculated as follows:

$$C_{BESS} = sign\, p_{BESS} \left| \left| \widetilde{P_{BESS}}(t) \right| - |P_{BESS}(t)| \right| \tag{18}$$

$$sign = \begin{cases} 1 & \forall t: \quad \Delta P_{\pm}\, P_{BESS}(t) \ge 0 \\ -1 & \forall t: \quad \Delta P_{\pm}\, P_{BESS}(t) < 0 \end{cases} \tag{19}$$

$$p_{BESS} = \quad \frac{CAPEX_{BESS}}{2 \quad Cycle_{BESS}\, E_n} \tag{20}$$

where $CAPEX_{BESS}$ is the BESS cost, while $Cycle_{BESS}$ is the number of charge-discharge cycles the storage system can endure before its end-of-life. Therefore, participation in the ancillary service market can entail additional costs for the FPU if the BESS use is increased with respect to self-consumption ($C_{BESS} > 0$), or savings if the BESS usage is reduced ($C_{BESS} < 0$).

It is worth highlighting that $\Delta Q_{\pm}$ regulation costs have not been considered, since these services are not yet addressed in the experimental initiatives motivating the present work [38], [39]. However, these costs could also be accounted for by using a framework similar to the one proposed here for $\Delta P_{\pm}$ regulation services.

If PV production curtailment is used to provide flexibility services to the grid, the cost of the regulation ΔP_{-} would correspond to the power exchanged with the grid $P_{M1}(t)$ at the time of the service provision. In this case, the flexibility cost would be a combination of the unsold PV production ΔP_{sale} at a price p_{sale} and the amount of energy purchased ΔP_{buy} at a price p_{buy}, as follows:

$$C_u = p_{sale} \quad \Delta P_{sale} + p_{buy} \quad \Delta P_{buy} \tag{21}$$

$$\Delta P_{sale} = \max(P_{M1}(t), 0) - \max\left(\widetilde{P_{M1}}(t), \quad 0\right) \tag{22}$$

$$\Delta P_{buy} = \min(P_{M1}(t), 0) - \min\left(\widetilde{P_{M1}}(t), \quad 0\right) \tag{23}$$

Note that this model also works for a stand-alone PV system, without a BESS connected to it, in which case, $P_{BESS}(t) = 0$ with the FPU just providing downward regulation by PV curtailment, i.e., $\Delta P_{-}^{\max}(t) = -P_{PV}(t)$ and $\Delta P_{+}^{\max}(t) = 0$, as per the corresponding capability curves in orange in Table 2.

3.2. CHP system

This system, illustrated in Fig. 5, produces electricity and heat in a cascade process, where the thermal energy q_{in} used to generate power P_{CHP} in the turbine (upper cycle) yields high-temperature heat, which can be recovered as useful energy q_{out} through a heat exchanger (bottom cycle) to supply thermal energy.

In this case, the flexibility potential of a CHP plant can be determined by assuming that q_{in} and P_{CHP} are known in advance. Thus, $\widetilde{P_{CHP}}$ can then be calculated as follows:

$$\widetilde{P_{CHP}}(t) = \quad P_{CHP}(t) + \Delta P_{CHP\pm} \tag{24}$$

$$P_{-}^{\max} \leq \quad \widetilde{P_{CHP}}(t) \leq P_{+}^{\max} \tag{25}$$

where $P_{+}^{\max}$ can be defined according to the capability curve of the turbine as illustrated in Table 2, while $P_{-}^{\max}$ is defined by the efficiency of the upper cycle η_{el}, which significantly decreases if P_{CHP} is low. Assuming that η_{el} monotonically increases with respect to P_{CHP} [40], the thermal energy variation Δq_{in} after an active power flexibility service can be defined as follows:

$$\Delta q_{in}(t) = \frac{\widetilde{P_{CHP}}(t)}{\eta_{el}(\widetilde{P_{CHP}}(t))} - \frac{P_{CHP}(t)}{\eta_{el}(P_{CHP}(t))} \tag{26}$$

On the other hand, q_{out} depends, within limits, on the bottom cycle efficiency η_{th}, η_{el}, and q_{in} as follows:

$$q_{out}(t) = \eta_{th}\,(1 - \eta_{el}(P_{CHP}(t)))\, q_{in}(t) \tag{27}$$

$$q_{out}^{\min} \quad \leq \quad \widetilde{q_{out}}(t) \leq q_{out}^{\max} \tag{28}$$

Hence, flexibility service activation impacts both q_{in} and q_{out}, where $q_{out}^{\min/\max}$ are chosen considering the user thermal comfort.

Assuming that before regulation, CHP covers the local electrical load, the system can provide both upward and downward regulation. For upward flexibility services ΔP_{+}, an increase in P_{CHP} results in a gain for the FPU equal to the difference between the price of the power delivered to the grid p_{sale} and the cost of the gas p_{gas} required to generate the additional q_{in}. On the other hand, for downward services ΔP_{-}, a reduction in P_{CHP} results in lost income equal to the power bought from the grid p_{buy} and the savings on gas. The CHP regulation costs can be defined as follows:

$$C_u: \quad \begin{cases} |\Delta P_{+}| & [p_{gas} - p_{sale}] \quad \forall \quad \Delta P_{+} \\ |\Delta P_{-}| & [p_{buy} - p_{gas}] \quad \forall \quad \Delta P_{-} \end{cases} \tag{29}$$

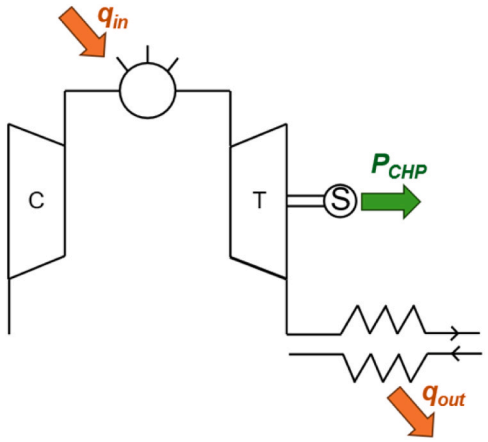

Fig. 5. CHP system.

4. Probabilistic aggregated regions

Once probabilistic FORs of each FPU are identified, these can be aggregated to quantitatively evaluate the amount of flexibility that a heterogeneous set of resources can provide. In this regard, it is proposed here to aggregate several FPUs to form PARs, which are of interest to several stakeholders, particularly BSPs, because of their many applications, such as evaluating DERs market potential, optimizing participation strategies, and designing resource portfolios. Moreover, by not directly embedding network constraints into the proposed PAR model, the developed statistical framework proves particularly advantageous for BSPs that can still estimate the aggregate flexibility potential of their contracted FPUs. Indeed, from the BSP standpoint adopted in this work, the methodology allows for estimating the aggregated flexibility potential without the need for full network observability, as BSPs typically have limited or no access to real-time distribution grid constraints. Consequently, the emphasis is placed on probabilistic resource availability, cost minimization, and service reliability, rather than on strict compliance with detailed operational network limits.

Given the probabilistic nature of the individual FORs, PARs must also incorporate information about the reliability of flexibility services provision. This is done through a Delivery Performance Index (DPI), which is defined as the % reliability of a set of aggregated DERs to provide a required flexibility service at a given instant, both for active and reactive power. A typical value for the DPI, adopted both in the literature and the experimental initiatives evaluating ancillary services from DERs, is 90% [31], [41].

To guarantee the required level of reliability, to produce the PAR, only $\Delta P_{\pm}$ and $\Delta Q_{\pm}$ variations with a service provision reliability higher than a specified DPI are considered. To this end, a Minkowski sum approach has been adopted to aggregate the individual FORs, as suggested in [25]. Hence, in a vector space, the Minkowski sum of the following two sets of points A and B is defined as the set of points obtained by adding the elements of A to those of B, as illustrated in Fig. 6. Once a specific DPI is specified, the vertices of each FOR are derived and vectors summed, as follows:

$$A \oplus B = \{a + b | a \in A \quad \wedge b \in B\} \tag{30}$$

It is worth noting that, although the adopted Minkowski-based aggregation is intentionally simplified, it remains efficient from a computational standpoint. Thus, the Minkowski sum is applied only to the DPI-filtered boundaries of each FOR in the aggregation, and the process is iterated for all DPI levels of interest. This selective aggregation significantly reduces the number of points involved in the computation, while still preserving the essential information encoded in the individual FORs, such as dynamic constraints and reliability. Furthermore, it is important to highlight that some technical limits at the grid's interface can be indirectly incorporated into the proposed numerical approach to

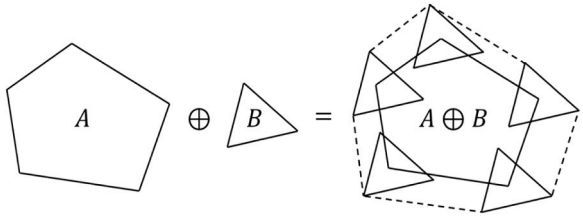

Fig. 6. Minkowski sum.

ensure that, for example, the provision of ancillary services to the HV system does not compromise grid operation. For instance, HV/MV transformer limits can be incorporated in the PAR resulting from the application of the Minkowski sum, further limiting the maximum exchangeable amount of active and reactive power. This approach is in line with the traffic light coordination mechanism widely adopted worldwide, aiming at enabling dynamic interaction between the transmission system and ADNs based on the operational status of the system [42]. Under green-light conditions, ancillary services can be requested by the TSO without limitations, while in yellow- and red-light conditions, ancillary services provision is still allowed but subject to constraints, or not allowed at all, respectively, to preserve system security.

Moreover, in order to evaluate the market opportunities and constraints associated with the ancillary services provision, service costs of the resulting PAR need to be considered in the methodology. Thus, for each $\Delta P_{\pm}$ variation, a sorting algorithm is implemented to determine which FPU may provide the required flexibility service at the lowest cost. Through a merit order approach, the algorithm prioritizes FPUs with the lower C_u to provide the required flexibility service.

5. Case study

In this Section, the proposed methodology is demonstrated and validated on four different case studies related to individual DERs and their aggregations. One of the key aspects of the presented work is the detailed description of the probabilistic FORs for individual FPUs, which is based on annual active and reactive power profiles from real PV systems located in Northern Italy, as described in detail in [43]. Furthermore, more than 100 non-flexible load profiles and CHP profiles have been derived from data gathered on real customers [44], using a 15 min resolution. In Fig. 7, an example of the active power profiles used for a PV plant and a CHP unit is illustrated for 4 representative days, one for each season. Note that the reliability of the DER service provision is inherently embedded in the proposed FORs; thus, the $CDF^{X}_{\pm}$ used to construct the FORs captures the natural variability of historical active and reactive measurements, including seasonal trends and operating fluctuations. Furthermore, the DPI index quantifies the reliability associated with each point inside PARs.

The first two scenarios described next are relevant to the identification of the probabilistic FORs of a PV power plant and a PV+BESS system, respectively. For the third case study, different FPUs are aggregated as an illustrative example of how the PAR is determined. Finally, the fourth case study involves the combination of distributed resources in a large portion of Milan's MV and LV distribution grid, considering more than 600 FPUs; in the latter, the traffic light coordination mechanism has been applied to demonstrate its application and impact on the resulting PAR.

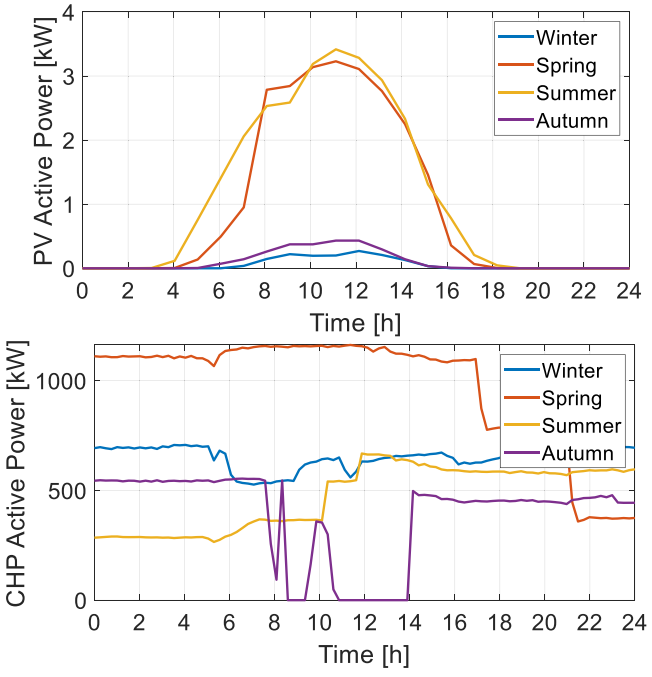

Fig. 7. PV and CHP active power profiles for four representative days.

5.1. Case 1: PV probabilistic FOR

This case study aims to investigate the reliability of an LV PV system in providing active and reactive flexibility services. As outlined in Section III, it is assumed that the FPU is designed to work at its optimal point, delivering its maximum active power. Given the absence of a storage system, the FPU can only offer downward regulation through PV curtailment, i.e., $P_{-}^{\max} = 0$. Thus, the profile of a residential PV system connected to the LV grid via a 4.4 kW inverter is analyzed next, where the capability is assumed to be of a TCC in Table 2 with $\cos\varphi_{\lim} = 0.9$, as per Italian technical standards for PV units of this size.

The reliability of the PV system in delivering flexibility services in each hour of the representative day in Summer is examined here. Fig. 8 illustrates the probabilistic FORs for 24 h, where the reliability of the FPU in providing active and reactive services is depicted with dark blue for the highest reliability, while dark red corresponds to the lowest one; observe that the FOR varies in both ΔP and ΔQ axes within $\Delta P_{-}^{\max}$ and $\Delta Q_{\pm}^{\max}$, versus reliability over time. Thus, from the 11 h to the 15 h, the PV unit can provide greater active and reactive flexibility, up to -3.30 kW and ± 1.40 kvar, respectively, due to the higher PV production, which enables a significant PV curtailment. On the other hand, when the PV production is lower, $\Delta P_{-}^{\max}$ and $\Delta Q_{\pm}^{\max}$ decrease, with non-zero FORs at the 7 h and the 19 h. Note also that as the curtailment ΔP_{-} increases, the capability of the FPU to deliver reactive power services decreases, which limits the FPU's ability to simultaneously provide both active and reactive power flexibility services.

Regarding the service provision reliability, the FORs calculated at the 11 h and the 15 h, even if similar in size, i.e., similar $\Delta P_{-}^{\max}$ and $\Delta Q_{\pm}^{\max}$, exhibit different reliability levels. Thus, considering a reliability index equal to or higher than 90 %, the first FOR yields $\Delta P_{-}^{\max} = 1.20$ kW, whereas the second one yields 1.90 kW. Therefore, the developed approach shows that the same PV power plant can provide a downward regulation ΔP_{-} with higher reliability at the 15 h than at the 11 h.

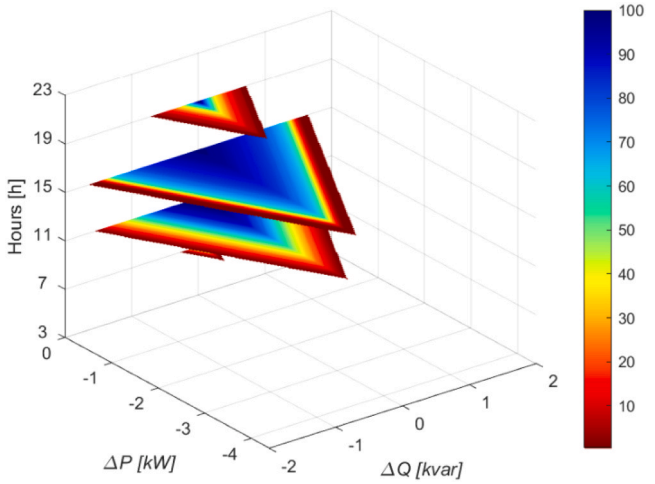

Fig. 8. Probabilistic FORs for a PV system over time in the Summer.

5.2. Case 2: PV+BESS probabilistic FOR

In this case study, a prosumer with a PV power plant and a BESS is considered during its operation on a Summer day. The PV panels and batteries are assumed to be connected to the grid by the same 4.4 kW power converter. The BESS technical characteristics are presented in Table 3 [45], [46]. The reactive power limits can be obtained from the capability curve TCC in Table 2 with a $\cos\varphi_{\text{lim}} = 0.9$ (areas colored in orange and green). For the BESS, realistic P_{BESS} and SoC profiles for the Summer are illustrated in Fig. 9, which were obtained by simulating the BESS charge/discharge according to PV production and load profiles extracted from the input database.

Fig. 10 shows the probabilistic FORs of the FPU with respect to Δt, where it can be observed that as the service duration increases, the size of the FOR decreases, reducing the FPU ability to deliver flexibility, in terms of both the provided regulation, i.e., $\Delta P_{\pm}^{\max}$ and $\Delta Q_{\pm}^{\max}$, and its reliability. Note that due to the limited energy capacity of the BESS, the probabilistic FOR is correlated to the duration of the service, i.e., the greater the service duration, the lower the service provision reliability that the BESS would be able to provide. For example, for an upward regulation ΔP_{+}, the greater the service duration, the greater the discharge of the batteries; hence, given that the batteries' SoC cannot be lower than $SoC^{\min}$, the BESS is able to supply a smaller amount of upward regulation as its duration increases. Thus, for $\Delta t = 1$ h, $\Delta P_{+}^{\max} = 4.30$ kW, while for $\Delta t = 5$ h, $\Delta P_{+}^{\max} = 1.25$ kW.

For downward regulation ΔP_{-}, the probabilistic FOR has a shape similar to that obtained in Case 1 for the 11 h to the 19 h, as illustrated in Fig. 8. This is because the FPU still provides services through PV curtailment, as the BESS contribution to downward regulation is limited by its SoC, which is close to $SoC^{\max}$. Since the BESS contributes to the regulation to a lesser extent, downward service provision is marginally affected by Δt. For both $\Delta P_{\pm}$ variations, the reactive limits $\Delta Q_{\pm}^{\max}$ of the probabilistic FOR follow the shape illustrated for a TCC in Table 2.

5.3. Case 3: PAR example

In this case study, an illustrative example is discussed of how different FORs can be aggregated into a PAR. Specifically, this case focuses on a simple flexibility perimeter that consists of three FPUs: a PV power plant, a BESS, and a PV+BESS system. In this scenario, the total capacity $\Delta P_{\pm}^{\max}$ and $\Delta Q_{\pm}^{\max}$, and DPI of the PAR are investigated under specific conditions, such as a required regulation duration. For the FPUs, the same power profiles and technical characteristics of the previous subsections have been assumed. In addition, the DPI threshold has been set at 90%, following the standards described in [38].

As an example, an ancillary service request is assumed here to be provided at the 13 h in the Summer, with a 1-hour service duration. For this scenario, Fig. 11 shows the probabilistic FORs of the individual FPUs considered. As expected, the PV system can only provide downward services, while the BESS and the PV+BESS unit can supply both downward and upward services. As highlighted in Case 2, the BESS contribution is limited due to its SoC value at this hour, which is close to $SOC^{\max}$.

To calculate the PAR, the individual FORs have been processed to ensure the reliability of the regulation provision above the minimum

Table 3
BESS technical characteristics.

Charging/Discharging Efficiency [%]	90
Maximum Discharging Power [kW]	4
Maximum Charging Power [kW]	3.5
Nominal Energy [kWh]	10
Minimum SoC [p.u.]	0.2
Maximum SoC [p.u.]	1
Number of Charging/Discharging Cycles	5000

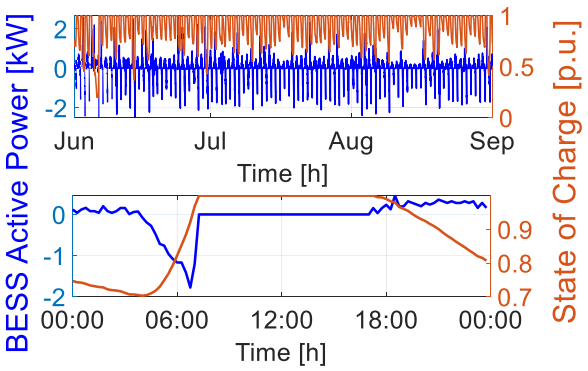

Fig. 9. BESS active power and SoC profiles in the Summer and for a specific day (July 15th).

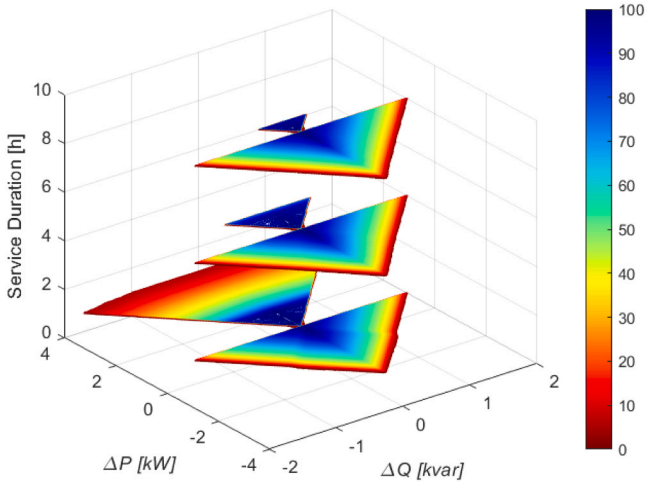

Fig. 10. Probabilistic FORs for a PV+BESS system in the Summer as a function of flexibility service duration.

90% DPI required by system operators (areas in blue in Fig. 11). Fig. 12 depicts the PAR resulting from this process based on the Minkowski sum. Note that this aggregation of FPUs can provide both upward and downward flexibility regulation, respectively, with $\Delta P_{+}^{\max} = 2.85$ kW and $\Delta P_{-}^{\max} = -3.95$ kW. The shape of the overall PAR results from the FPU's TCC capability curve in Table 2. Moreover, if no active power regulation is supplied to the grid, i.e., $\Delta P_{\pm} = 0$, the FPUs' aggregate can provide a consistent $\Delta Q_{\pm} = \pm 1.39$ kvar. On the other hand, if a ΔP_{+} close to $\Delta P_{+}^{\max}$ is provided, the aggregate can deliver a reactive power contribution $\Delta Q_{\pm} = \pm 1.30$ kvar. The maximum reactive power that can be provided by the FPU aggregate drops to ± 0.48 kvar for a ΔP_{-} close to $\Delta P_{-}^{\max}$.

5.4. Case 4: PAR application to a real urban scenario

This case study aims to demonstrate the potential of the PAR concept in a real scenario, relevant to the power distribution network of the metropolitan area of Milan. To this end, the actual DERs connected to the 25 MVA transformer of an HV/MV substation have been considered as per Table 4, where the numbers and types of power plants, as well as the total installed capacity by voltage level, have been extracted from the Development Plan of Unareti [47], Milan's DSO. In the area considered, a total BESS's energy capacity of 2 MWh is installed; however, since no information regarding the battery's energy capacity of the individual FPU is available, an Energy to Power Ratio (EPR) value equal to 2 has been assumed for all BESS. Regarding the CHP units' technical

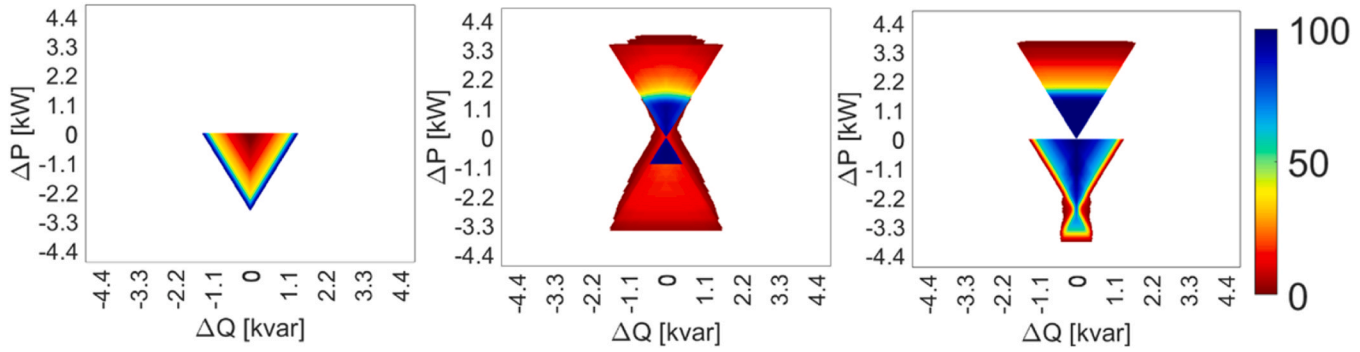

Fig. 11. Probabilistic FORs of a PV, BESS, and PV+BESS for the Summer day at the 13 h.

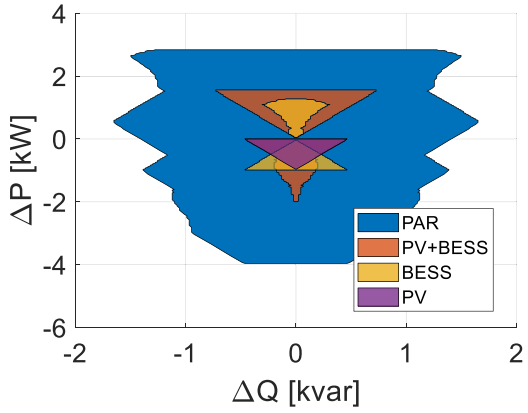

Fig. 12. PAR of three aggregated FPUs and a 90% DPI.

Table 4
Case 4 DERs.

Voltage level	Type	Capability curve	Number	Total installed power [MVA]
LV	PV	TCC	462	1.828
		RCC	94	4.370
	PV+BESS	TCC	51	0.234
		RCC	10	0.266
	CHP	SCC	8	0.210
MV	PV	LCC	6	0.653
		CCC	2	2.092
	PV+BESS	LCC	2	0.500
	CHP	SCC	6	3.570

limits, it has been assumed that $\cos\varphi_{\text{lim}} = 0.98$, $P_{+}^{\max} = 0.8S_n$, $P_{-}^{\max} = 0$, and $q_{out}^{\min/\max} = \pm 0.1\, q_{out}(t)$ [35]. The CHP electrical efficiency has been modeled according to the characteristic in Fig. 13, with $\eta_{th} = 0.9$ [40].

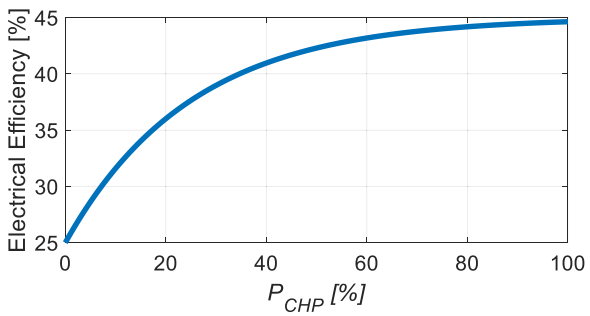

Fig. 13. Electrical efficiency of CHP units.

5.4.1. PAR computation

In a similar fashion to the previous case studies, and in response to a more stressed condition caused by increased air conditioning loads on Milan's grid, the PARs are derived for the 13 h with a 1-hour duration for the FPUs listed in Table 4, as illustrated in Fig. 14. The resulting LV and MV PARs highlight that the proposed methodology enables BSPs to rapidly and reliably quantify the amount of flexibility that can be committed to market services, even in the absence of complete knowledge of network topology and operational constraints. By focusing on probabilistic resource availability, service reliability, and cost efficiency, BSPs can make informed market participation decisions without the need for detailed grid feasibility studies, which typically fall under the DSO's responsibility.

In this regard, observe that as the DPI varies from 50 to 90%, the $\Delta P_{\pm}^{\max}$ and $\Delta Q_{\pm}^{\max}$ values change, with the LV and MV PARs showing different contributions to the flexibility provision. This is due to the different mix of DER's technologies at the two voltage levels, given the considerable number of large CHP units connected to the MV grid that add up to 3570 kW, plus the limits imposed by the relevant capability curves. Furthermore, the LV PAR indicates that LV FPUs can provide greater downward regulation than upward regulation, due to the prevalence of PV systems at this level and limited availability of BESSs.

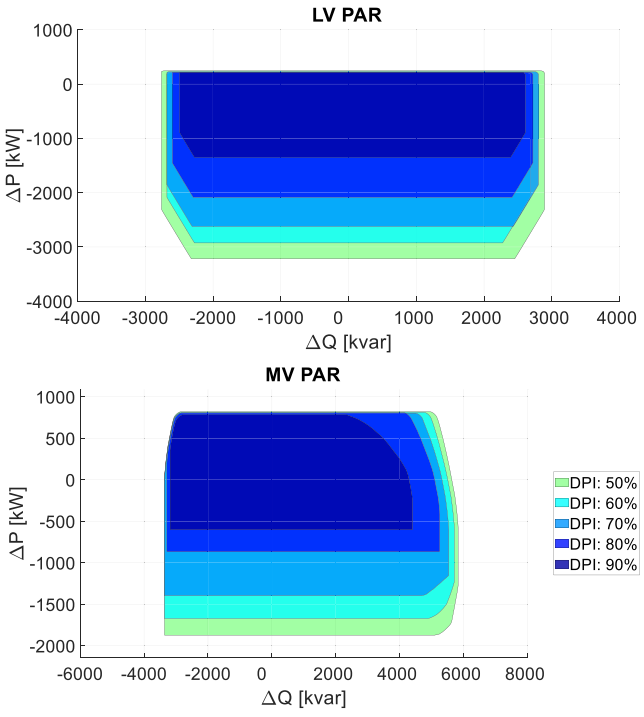

Fig. 14. PARs of LV and MV FPUs for the studied portion of Milan' grid.

Regarding the provision of reactive power services, as downward regulation ΔP_{-} increases, $\Delta Q_{\pm}^{\max}$ provision initially remains constant, following the shape of the RCC capability curve in Table 2, with $\Delta Q_{\pm}^{\max}$ decreasing afterwards, following the profile of the TCC capability curve. In this regard, for a 60% DPI, $\Delta Q_{\pm}^{\max} = \pm 2624$ kvar remains constant until ΔP_{-} reaches -1940 kW. On the other hand, for a 90% DPI, $\Delta Q_{\pm}^{\max} = \pm 2470$ kvar remains constant until ΔP_{-} reaches -838 kW. In addition, note that $\Delta P^{\max}$ is strongly influenced by the DPI, since for a reliability of 60%, $\Delta P_{-}^{\max} = -3090$ kW, while for 90%, $\Delta P_{-}^{\max} = -1247$ kW.

The MV PAR shows that MV FPUs can provide greater upward services than LV ones, with $\Delta P_{+}^{\max} = 790$ kW for a 60% DPI. Furthermore, the availability of CHP units at the MV level also affects the provision of reactive regulation, with significant $\Delta Q_{\pm}^{\max}$ values for capacitive and inductive services due to the stability limit of the CPU synchronous generators, as per the SCC capability curve in Table 2. Thus, as the DPI increases from 50 to 80%, $\Delta Q_{\pm}^{\max}$ remains almost constant at -3290 and 5250 kvar, respectively.

5.4.2. Grid limits

Some technical grid limits, such as limits on the HV/MV transformer interface, can be explicitly incorporated in the proposed approach based on a traffic light coordination mechanism. These limits can be communicated by the grid operator (e.g., the DSO) to the BSP, which can consider them in the PAR definition. An illustrative example of this approach is shown in Fig. 15 for June 6, 2024. Thus, the preexisting operating condition at the HV/MV transformer with no ancillary service provision is depicted as a red dot in the figure, corresponding to a power absorption from the distribution grid of 22 MW at a lagging power factor of 0.98, while the transformer power constraints are represented as an arc centered on the axes origin for an assumed power capacity of 25 MVA, which is a typical rated power of HV/MV transformers in Italy. Thus, the amount of flexibility that the DERs available on the ADN can supply to the TSO is equal to the intersection of the PAR and the maximum transfer capacity limit of the transformer interface. In the scenario under analysis, for example, the downward regulation ΔP_{-} is constrained, with any additional increase in consumption or a corresponding reduction in local generation potentially exceeding the 25 MVA capacity of the transformer.

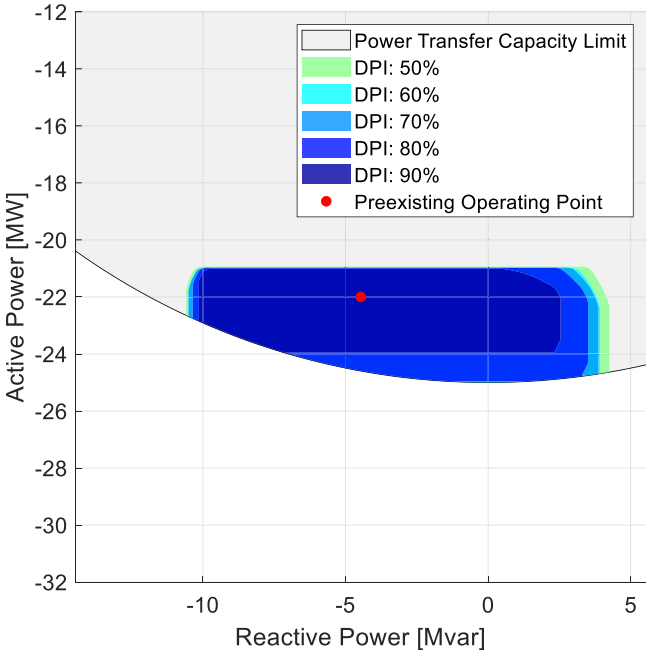

Fig. 15. PAR at the TSO-DSO interface subject to technical constraints.

5.4.3. Flexibility service costs

To study the cost of flexibility service provision, it is assumed that $p_{buy} = 0.30$ €/kWh and $p_{sale} = 0.11$ €/kWh, with the former corresponding to the 2024 average of the Italian energy retail prices, while the latter corresponds to the 2024 average of the day-ahead zonal prices for Central-North Italy [48]. The p_{BESS} value has been calculated considering a $CAPEX_{BESS} = 500$ €/kWh, and $Cycle_{BESS} = 5000$. Finally, a $p_{gas} = 0.18$ €/kWh has been used, which corresponds to the 2023 average of Italian gas retail prices, considering an average gas turbine efficiency of 0.35 [48].

To evaluate the potential of DERs in participating in ancillary service markets, the service costs of the resulting LV and MV PARs have been sorted using a merit order algorithm. This yields the FPUs' $\Delta P_{\pm}^{\max}$ and associated flexibility costs in €/kWh depicted in Fig. 16 for a 60% and 90% DPI. Observe that, for both LV and MV PARs, reliability significantly impacts the FPUs downward contributions, i.e., the maximum share of ΔP_{-}, and consequently the flexibility costs. For MV FPUs with a 60% DPI, the DSO can require a $\Delta P_{-} = -1300$ kW with a flexibility cost of 0.11 €/kWh, whereas with a 90% DPI, the downward contribution is reduced to -600 kW for the same unit cost. Note, on the other hand, that upward regulation is less affected by an increase in the reliability index, with more constant flexibility costs. Thus, for instance, the minimum relative cost that grid operators need to pay is 0.07 €/kWh for $\Delta P_{+} = 600$ kW from MV FPUs, whereas, for a greater upward regulation, they would have to purchase flexibility from other DERs with higher flexibility costs, such as PV+BESS systems at 0.225 €/kWh. Finally, it is worth noticing that fewer FPUs can provide upward regulation, due to the presence of several PV systems with a $\Delta P_{+}^{\max} = 0$.

5.4.4. Scalability and computational performance for large BSP portfolios

The last case study shows that the proposed methodology is inherently scalable and computationally tractable for large BSP portfolios. Thus, the computation of probabilistic FORs relied on metering-based distributions and can be performed independently for each FPU (before service delivery), enabling full parallelization across several DERs. In addition, the aggregation process used to construct PARs adopts a DPI-filtered Minkowski sum, which bounds the growth of boundary vertices and avoids exponential complexity. This design ensures that the overall framework remains efficient and applicable even for portfolios comprising several hundred FPUs connected to the same HV/MV node, ensuring that the computational effort observed in the case studies is representative of practical BSP operations.

Regarding computational burdens, the numerical calculations of the PARs described in this section required 270 s. These were performed in a MATLAB environment on a 12th Generation Intel(R) Core (TM) i7–1255U, CPU 1.70 GHz, RAM 16 GB computer.

6. Conclusions

This paper introduced the concept of probabilistic FOR to assess the flexibility potential of a heterogeneous set of FPUs through active-reactive power regions that describe the DER's reliability to provide flexibility services. By incorporating capability limits, service duration and dynamic constraints, the proposed statistical framework enables BSPs to characterize the availability of individual FPUs without requiring real-time measurements or full network observability. The methodology was extended to sets of aggregated resources through the definition of PARs, obtained via a DPI-filtered Minkowski sum that preserves reliability while remaining computationally efficient for large BSP portfolios. This provides a practical tool for assessing market potential, supporting bidding strategies, and constructing cost-optimal portfolios of DERs.

The numerical studies, covering individual FPUs, mixed portfolios, and a real urban network, demonstrated that probabilistic FORs offer a more informative description of DER flexibility than deterministic

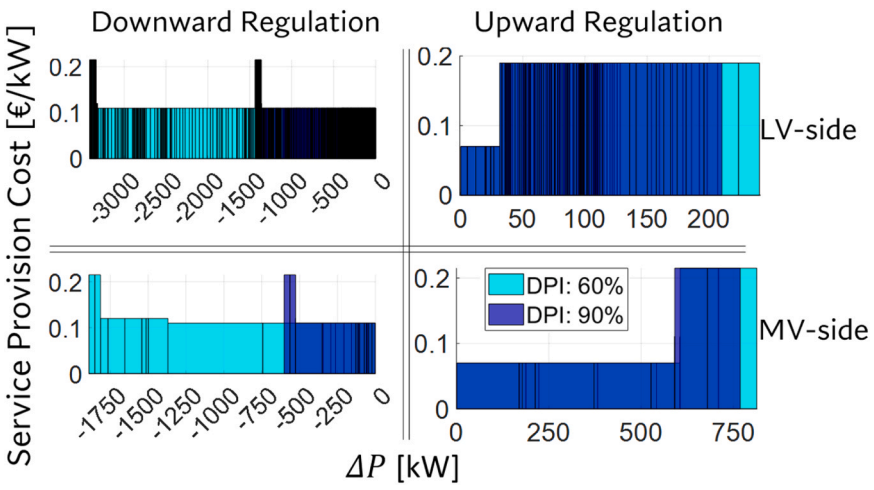

Fig. 16. Downward and upward flexibility costs of LV and MV PARs with 60% and 90% DPI.

approaches. In particular, the large-scale case study based on the Milan distribution network showed that the proposed framework can efficiently handle the aggregation of more than 600 DERs connected to the same HV/MV substation, with LV and MV PARs computed in the order of seconds. This confirms the scalability and practical applicability of the proposed methodology for BSP operations, both at the distribution level and across the TSO–DSO interface, even under limited grid observability.

Possible limitations of the developed methodology include the computation of empirical *CDF*s requiring representative historical active and reactive measurements, which may not be available for newly installed DERs or in poorly monitored networks. Moreover, since the approach is designed for contexts where BSPs operate with limited or no grid information, grid's constraints are not explicitly accounted by FORs, although external constraints provided by DSOs can be incorporated in a simplified form. For these reasons, future works could focus on hybrid approaches that integrate probabilistic FORs and PARs with network's constraints, considering the computational burden associated with large-scale BSP portfolios, while accounting for scenarios in which DERs active and reactive power measurements are incomplete or unavailable.

Funding

This work has been supported by the National Recovery and Resilience Plan (PNRR), Mission 4, Component 2 ("From Research to Business"), in accordance with DM 352 of April 04, 2022.

CRediT authorship contribution statement

Edoardo Daccò: Writing – review & editing, Writing – original draft, Visualization, Software, Methodology, Investigation, Formal analysis, Data curation, Conceptualization. **Claudio Cañizares:** Writing – review & editing, Visualization, Validation, Supervision, Conceptualization. **Davide Falabretti:** Writing – review & editing, Writing – original draft, Supervision, Project administration, Methodology, Investigation, Formal analysis, Data curation, Conceptualization.

Declaration of Competing Interest

The authors declare that they have no known competing financial interests or personal relationships that could have appeared to influence the work reported in this paper.

Data availability

Data will be made available on request.

References

[1] European CommissionEuropean Commission, NextGenerationEU: A recovery plan for Europe, 2021. Available: https://ec.europa.eu/info/strategy/recovery-plan-europe_en.2021.
[2] European Commission, Fit for 55: Delivering the EU's 2030 climate target on the way to climate neutrality, 2021. Available: ⟨https://eur-lex.europa.eu/legal-content/EN/TXT/HTML/?uri=CELEX%3A52021DC0550⟩.
[3] International Energy Agency (IEA) , Unlocking the potential of distributed energy resources: power system opportunities and best practices, Paris, France, 2022. Available: ⟨https://iea.blob.core.windows.net/assets/3520710c-c828-4001-911c-ae78b645ce67/UnlockingthePotentialofDERs_Powersystemopportunitiesandbestpractices.pdf⟩.
[4] European Union, Directive 2019/944 of the European parliament and of the council on common rules for the internal market for electricity, 2019. Available: ⟨https://eur-lex.europa.eu/eli/dir/2019/944/oj⟩.
[5] Energy Networks Association, Open networks project: opening markets for flexibility, 2017. Available: ⟨https://www.energynetworks.org/creating-tomorrows-networks/open-networks⟩.
[6] ARERA, Resolution 352/2021/R/EEL pilot projects for the procurement of local ancillary services, 2021. Available: ⟨https://www.arera.it⟩.
[7] I. Sperstad, M. Degefa, G. Kjølle, The impact of flexible resources in distribution systems on the security of electricity supply: a literature review, Electr. Power Syst. Res. 188 (2020) 106532.
[8] N. Pourghaderi, M. Fotuhi-Firuzabad, M. Moeini-Aghtaie, M. Kabirifar, P. Dehghanian, A local flexibility market framework for exploiting DERs' flexibility capabilities by a technical virtual power plant, IET Renew. Power Gener. 17 (2023) 681–695.
[9] M. Zeraati, et al., A novel state estimation method for distribution networks with low observability based on linear AC optimal power flow model, Electr. Power Syst. Res. 228 (2024).
[10] F. Gulotta, E. Daccò, A. Bosisio, D. Falabretti, Opening of ancillary service markets to distributed energy resources: a review, Energies 16 (6) (2023).
[11] P. Cuffe, P. Smith, A. Keane, Capability chart for distributed reactive power resources, IEEE Trans. Power Syst. 29 (1) (2014) 15–22.
[12] S. Bruno, Mapping flexibility region through three-phase distribution optimal power flow at TSO-DSO point of interconnection, in: Proc. AEIT, Milan, Italy, 2021, pp. 1–6..
[13] W. Lin, Y. Wang, J. Wu, F. Feng, Model-free aggregation for virtual power plants using input convex neural networks, IEEE Trans. Smart Grid.
[14] X. Jiang, Y. Zhou, W. Ming, J. Wu, Feasible operation region of an electricity distribution network, Appl. Energy 331 (2023) 120419.
[15] F. Capitanescu, TSO–DSO interaction: active distribution network power chart for TSO ancillary services provision, Electr. Power Syst. Res. 163A (2018) 226–230.
[16] S. Riaz, P. Mancarella, On Feasibility and Flexibility Operating Regions of Virtual Power Plants and TSO/DSO interfaces, in: IEEE PowerTech, Milan, Italy, 2019, pp. 1–6.
[17] A. Churkin, Impacts of distribution network reconfiguration on aggregated DER flexibility, in: IEEE Belgrade PowerTech, Serbia, 2023, pp. 1–7.
[18] D.A. Contreras, K. Rudion, Computing the feasible operating region of active distribution networks: Comparison and validation of random sampling and optimal power flow based methods, IET Gener. Transm. Distrib. 15 (10) (2021) 1600–1612.

[19] A. Churkin, W. Kong, J.N. Melchor Gutierrez, E.A. Martínez Ceseña, P. Mancarella, Tracing, ranking and valuation of aggregated DER flexibility in active distribution networks, IEEE Trans. Smart Grid 15 (2) (2024) 1694–1711.
[20] D.A. Contreras, K. RudionImproved assessment of the flexibility range of distribution grids using linear optimization, In: Proceedings of the PSCC, Dublin, Ireland, 2018, pp. 1–7.
[21] G. Papazoglou, P. Biskas, Review of methodologies for the assessment of feasible operating regions at the TSO–DSO interface, Energies 15 (14) (2022).
[22] G.K. Papazoglou, Estimating the feasible operating region of active distribution networks using the genetic algorithm, In: Proceedings of the IEEE PES GTD, Istanbul, Turkiye, 2023, pp. 182–187.
[23] R. Nebuloni, Optimal management of flexibility services in LV distribution grids, in: CIRED, Rome, Italy, 2023, pp. 2034–2038..
[24] H. Früh, et al., Coordinated vertical provision of flexibility from distribution systems, IEEE Trans. Power Syst. 38 (2) (2023) 1834–1844.
[25] S. Riaz, P. Mancarella, Modelling and characterisation of flexibility from distributed energy resources, IEEE Trans. Power Syst. 37 (1) (2022) 38–50.
[26] J. Naughton, et al., Optimization of multi energy virtual power plants for providing multiple market and local network services, Electr. Power Syst. Res. 189 (2020).
[27] Y. Zou, Y. Xu, "DER-inverter based reactive power ancillary service for supporting peer-to-peer transactive energy trading in distribution networks, IEEE Trans. Power Syst. 40 (1) (Jan. 2025) 753–764.
[28] J. Silva, et al., Estimating the active and reactive power flexibility area at the TSO–DSO interface, IEEE Trans. Power Syst. 33 (5) (2018) 4741–4750.
[29] M. Sarstedt, L. Hofmann, Monetarization of the feasible operation region of active distribution grids based on a cost-optimal flexibility disaggregation, IEEE Access 10 (2022) 5402–5415.
[30] S. Stanković, L. Söder, Probabilistic reactive power capability charts at DSO/TSO interface, IEEE Trans. Smart Grid 11 (5) (2020) 3860–3870.
[31] A. Churkin, Assessing distribution network flexibility via reliability-based P–Q area segmentation, In: Proceedings of the IEEE Belgrade PowerTech, Serbia, 2023, pp. 1–6.
[32] X. Liu, et al., Dynamic aggregation strategy for a virtual power plant to improve flexible regulation ability, Energy 297 (2024).
[33] ENTSO-E, EDSO, An integrated approach to active system management, Apr. 2019. Available: ⟨https://eepublicdownloads.entsoe.eu/clean-documents/Publications/Position%20papers%20and%20reports/TSO-DSO_ASM_2019_190416.pdf⟩.
[34] A. Patig, O. Stanojev, P. Aristidou, A. Kiprakis, G. Hug, Fast Mapping of Flexibility Regions at TSO-DSO Interfaces under Uncertainty, in: IEEE ISGT-Europe, Novi Sad, Serbia, 2022, pp. 1–6.
[35] Italian Electrotechnical Committee, CEI 0-16: Reference technical rules for the connection of active and passive consumers to the HV and MV electrical networks of distribution company, 2019. Available: ⟨https://mycatalogo.ceinorme.it/cei/item/0000016796?sso=y⟩.
[36] Italian Electrotechnical Committee, CEI 0-21: Reference technical rules for the connection of active and passive users to the LV electrical utilities, 2022. Available: ⟨https://mycatalogo.ceinorme.it/cei/item/0000016797?sso=y⟩.
[37] A. Scrocca, E. Daccò, D. Andreotti, G. Rancilio, F. Bovera, D. Falabretti, M. Delfanti, Local flexibility markets in Europe: a critical review of market designs, operational maturity and stakeholder perspectives, Renew. Sustain. Energy Rev. 226 (Part D) (2026) 116434.
[38] Unareti, MiNDFlex project, Pilot project on smart grid flexibility management, 2024. Available: ⟨https://www.unareti.it/it/media/progetti/sperimentazione-mindflex-rete-elettrica-milano⟩.
[39] Terna Sp.A., Regulation governing the methods for creation, qualification and management of enabled consumption virtual units (UVAC) to the ancillary service market, 2017. Available: ⟨https://download.terna.it/terna/0000/0930/30.PDF⟩.
[40] C. Milan, et al., Modeling of non-linear CHP efficiency curves in distributed energy systems, Appl. Energy 148 (2015) 334–347.
[41] Terna, Approvvigionamento a termine di risorse di dispacciamento per i soggetti titolari di unità virtuali abilitate miste (UVAM) al mercato dei servizi di dispacciamento, 2021. Available: ⟨https://download.terna.it/terna/Procedura%20per%20approvvigionamento%20a%20termine%20UVAM_2023_POST%20CONSULTAZIONE_clean_8db977568f616b2.pdf⟩.
[42] Terna, Traffic Light Model for dynamic TSO-DSO coordination in the management of flexibility resources in distribution networks – Technical report, 2022. Available: ⟨https://download.terna.it/terna/Relazione_Tecnica_TSO_DSO_consultazione_aggiornamento_8db038d82a98385.pdf⟩.
[43] F. Gulotta, et al., Short-term uncertainty in the dispatch of energy resources for VPP: a novel rolling horizon model based on stochastic programming, Int. J. Electr. Power Energy Syst. 153 (2023).
[44] L. Pellegrino, C. SandroniAggregation of residential energy storage systems, in: AEIT, Florence, Italy, 2019, pp. 1–6..
[45] H. Jaffal, et al., Battery energy storage system performance in providing various electricity market services, Batteries 10 (3) (2024).
[46] D. Falabretti, F. Gulotta, D. Siface, Scheduling and operation of RES-based virtual power plants with e-mobility: a novel integrated stochastic model, Int. J. Electr. Power Energy Syst. 144 (2023) 108604.
[47] Unareti, Development plan 2023, 2023. Available: ⟨https://www.unareti.it/it/chi-siamo/informazioni-servizio/piano-sviluppo-incremento-resilienza⟩.
[48] Italian Electricity Market Operator, Mercati Elettrici, 2024..